

ORIGINAL ARTICLE

Blockade of the K_{ATP} channel Kir6.2 by memantine represents a novel mechanism relevant to Alzheimer's disease therapy

S Moriguchi¹, T Ishizuka², Y Yabuki¹, N Shioda¹, Y Sasaki¹, H Tagashira¹, H Yawo², JZ Yeh³, H Sakagami⁴, T Narahashi³ and K Fukunaga¹

Here, we report a novel target of the drug memantine, ATP-sensitive K^+ (K_{ATP}) channels, potentially relevant to memory improvement. We confirmed that memantine antagonizes memory impairment in Alzheimer's model APP23 mice. Memantine increased CaMKII activity in the APP23 mouse hippocampus, and memantine-induced enhancement of hippocampal long-term potentiation (LTP) and CaMKII activity was totally abolished by treatment with pinacidil, a specific opener of K_{ATP} channels. Memantine also inhibited Kir6.1 and Kir6.2 K_{ATP} channels and elevated intracellular Ca^{2+} concentrations in neuro2A cells overexpressing Kir6.1 or Kir6.2. Kir6.2 was preferentially expressed at postsynaptic regions of hippocampal neurons, whereas Kir6.1 was predominant in dendrites and cell bodies of pyramidal neurons. Finally, we confirmed that Kir6.2 mutant mice exhibit severe memory deficits and impaired hippocampal LTP, impairments that cannot be rescued by memantine administration. Altogether, our studies show that memantine modulates Kir6.2 activity, and that the Kir6.2 channel is a novel target for therapeutics to improve memory impairment in Alzheimer disease patients.

Molecular Psychiatry advance online publication, 25 October 2016; doi:10.1038/mp.2016.187

INTRODUCTION

Alzheimer's disease (AD) is a progressive neurodegenerative disorder characterized by cognitive deficits and memory loss. The brains of AD patients reportedly show reduced activity of *N*-methyl-D-aspartate receptor (NMDAR) and down-regulation of cholinergic systems.¹ Memantine, which is approved by the Food and Drug Administration for clinical use in AD, acts as a noncompetitive, moderate-affinity antagonist of NMDAR channels.² Memantine binds near the Mg^{2+} binding site of those channels,³ and its moderate blocking activity apparently relieves excessive glutamate-induced synaptic 'noise' in AD patients. Such NMDAR inhibition by memantine ameliorates glutamate toxicity, slowing further progressive neuronal cell death due to amyloid- β ($A\beta$) proteins.⁴ However, mechanisms underlying improved cognitive function in memantine-treated AD patients remains unclear. Ca^{2+} /calmodulin-dependent protein kinase II (CaMKII) signaling is downstream of NMDAR,⁵ and CaMKII is a critical kinase for NMDAR- and hippocampus-dependent memory formation.⁶ Initially, we observed that, in addition to blocking NMDAR channels, memantine administration elevates CaMKII activity *in vivo*, suggesting that it improves memory via a novel mechanism.

ATP-sensitive K^+ (K_{ATP}) channels are widely distributed in brain and comprised of four identical (either Kir6.1 or Kir6.2) inwardly rectifying K^+ channel subunits plus four identical (either SUR1, SUR2A or SUR2B) high-affinity sulphonylurea receptor subunits in peripheral tissues and brain.⁷ K_{ATP} channels are expressed in various subunit combinations, such as SUR1-Kir6.1, SUR1-Kir6.2 or SUR2-Kir6.2 in hippocampal pyramidal cells or SUR1-Kir6.2 in hippocampal interneurons.⁸ In brain, Kir6.2 is predominant in neurons and exerts critical roles in glucose sensing and neuronal

excitability in response to metabolic demands.⁹ By contrast, Kir6.1 is primarily expressed in glial cells, such as astrocytes or microglia, and has a less critical role in adult neurogenesis.¹⁰ We previously documented that small conductance Ca^{2+} -activated K^+ (SK) channels are novel targets for phosphorylation by CaMKII in Junctophilin null mice,¹¹ which exhibit memory impairment. Junctophilin is a structural protein associated with the endoplasmic reticulum and critical for bridging NMDAR and SK channels in hippocampal synaptic membranes.¹¹ Junctophilin loss increases NMDAR-dependent CaMKII activity, suggesting that K^+ channel regulation by NMDAR is critical for hippocampus-dependent memory and CaMKII regulation and that, by extension, memantine targets K^+ channels in brain.

Here, we show novel functions of Kir6.2 in synaptic plasticity and report that Kir6.2 activities are directly regulated by memantine. As changes in diverse diabetes-related genes are seen in AD brains,¹² memantine-regulated K_{ATP} channels now represent a novel therapeutic target to antagonize memory loss in diabetes and AD patients.

MATERIALS AND METHODS

Study approval

All animal procedures were approved by the Committee on Animal Experiments at Tohoku University and are based on based NIH guidelines.

Generation of mutant or transgenic mice

Kir6.1 +/- and *Kir6.2* -/- mice. *Kir6.1* +/- mice were generated by targeted disruption of the *KCNJ8* gene. Mice were backcrossed for more than 10 generations onto a C57BL/6J background. *Kir6.2* -/- mice were generated by targeted disruption of the corresponding gene and similarly backcrossed onto a C57BL/6J background. For a detailed protocol for both

¹Department of Pharmacology, Graduate School of Pharmaceutical Sciences, Tohoku University, Sendai, Japan; ²Department of Developmental Biology and Neuroscience, Graduate School of Life Sciences, Tohoku University, Sendai, Japan; ³Department of Molecular Pharmacology and Biological Chemistry, Northwestern University Feinberg School of Medicine, Chicago, IL, USA and ⁴Department of Anatomy, Kitasato University School of Medicine, Sagami-hara, Japan. Correspondence: Professor K Fukunaga or Dr S Moriguchi, Department of Pharmacology, Graduate School of Pharmaceutical Sciences, Tohoku University, 6-3 Aramaki-Aoba, Aoba-ku, Sendai, Miyagi 980-8578, Japan. E-mail: kfukunaga@m.tohoku.ac.jp or shigeki@m.tohoku.ac.jp

Received 24 December 2015; revised 11 August 2016; accepted 22 August 2016

procedures see Miki et al.^{13,14} Kir6.2 +/- mice were made by crossing Kir6.2 -/- mice and wild-type mice. Kir6.1 +/- mice and Kir6.2 -/- mice (both male) 8–10 weeks of age were used in experiments.

APP23 transgenic mice

APP23 transgenic mice, which express mutant human-type APP (Swedish double mutation) under the murine brain and neuron-specific murine Thy-1 promoter, were provided by Novartis Pharma (Nervous System Research, Basel, Switzerland). Details relevant to their construction are found in Sturchler-Pierrat et al.¹⁵ APP23 mice and wild-type mice (both male) 12–14 months of age were used in experiments.

CaMKIIa +/- mice. CaMKIIa +/- mice (strain B6;129P2-CaMKII2a/J) were obtained from the Jackson Laboratory (Bar Harbour, ME, USA). Here, we used heterozygous CaMKIIa mice bred for more than 20 generations on a C57BL/6J background and continuously backcrossed on that strain thereafter. Mice were housed one per cage after weaning. Details relevant to mouse construction are provided by Yamasaki et al., 2008.¹⁶ CaMKIIa +/- mice (male) 8–10 weeks of age were used in experiments.

CaMKIV -/- null mice. CaMKIV -/- null mice were provided from Prof. Hiroyuki Sakagami at Kitasato University. To disrupt the CaMKIV gene, the exon containing the initiation codon was replaced with a neomycin resistance cassette. Southern blot analysis using a 3' external probe confirmed homologous recombination in CCE embryonic stem (ES) cells derived from the 129/SvJ mouse strain. A detailed protocol is provided by Takao et al.¹⁷ CaMKIV -/- null mice (male) 8–10 weeks of age were used in experiments.

Behavioral tests

Y-maze task. Spontaneous alternation behavior in a Y-maze was assessed as a spatial reference memory task. The apparatus consisted of three identical arms (50 × 16 × 32 cm) made of black plexiglas. Mice were placed at the end of one arm and allowed to move freely through the maze during an 8-min session. The sequence of arm entries was recorded manually. An alternation was defined as entries into all three arms as consecutive choices. The maximal number of alternations was thus the total number of arms entered minus two, and the percentage of alternations was calculated as actual alternations/maximum possible alternations × 100. In addition, the total number of arms entered during a session was also determined.

Novel object recognition task. This task is based on the tendency of rodents to discriminate a familiar from a new object. Mice were individually habituated to an open-field box (35 × 25 × 35 cm) for 2 consecutive days. The experimenter scoring behavior was blinded to the treatment. During the acquisition phases, two objects of the same material were placed in a symmetric position in the center of the chamber for 5 min. One hour later, one object was replaced by a novel object, and exploratory behavior was analyzed for 5 min. After each session, objects were thoroughly cleaned with 75% ethanol to prevent odor recognition. Exploration of an object was defined as rearing it or sniffing it at a distance of less than 1 cm, touching it with the nose, or both. Successful recognition of a previously explored object was reflected by preferential exploration of the novel object. Discrimination of spatial novelty was assessed by comparing the difference in time spent exploring the novel versus the familiar object. Total time spent exploring both objects was also recorded to allow adjustment for differences in total exploration time.

Step-through passive avoidance task. Training and retention trials of the passive avoidance task were conducted in a box consisting of dark (25 × 25 × 25 cm) and light (14 × 10 × 25 cm) compartments with a floor constructed of stainless steel rods. Rods in the dark compartment were connected to an electronic stimulator (Nihon Kohden, Tokyo, Japan). Mice were habituated to the apparatus the day before passive avoidance acquisition. On training trials, a mouse was placed in the light compartment, and when the mouse entered the dark compartment, the door was closed and the mouse received an inescapable electric shock (1 mA for 500 ms) through the floor grid and then removed from the apparatus 30 s later. The same procedure without footshock was repeated after 24 h to assess retention levels. The time before entering the dark chamber within 300 s (as the maximum time) was recorded after animals were returned to the light chamber.

Cell culture and transfection

Neuro2A (N2A) cells were cultured in Dulbecco's modified Eagle's medium (DMEM) (Invitrogen, Carlsbad, CA, USA) containing 10% fetal bovine serum at 37 °C with 5% CO₂. Cells were plated in 35 mm dishes, cultured in standard medium for 24-h, and then transfected with 2 µg ml⁻¹ of plasmids encoding Kir6.1 or Kir6.2 with lipofectamine 2000 (Invitrogen) in 0.5 ml of serum-free medium for 6-h. Medium was then changed to standard medium, and cells were cultured an additional 48-h.

Electrophysiology

Extracellular recording. Brains were rapidly removed from ether-anesthetized male mice (C57BL/6J) and hippocampi dissected out. Transverse hippocampal slices (400 µm thick) prepared using a vibratome (Leica VT1000S, Leica Microsystems, Wetzlar, Germany) were incubated for 2-h in continuously oxygenated (95% O₂, 5% CO₂) artificial cerebrospinal fluid (ACSF) at room temperature (28 °C). After a 2-h recovery period, a slice was transferred to an interface recording chamber and perfused at a flow rate of 2 ml min⁻¹ with ACSF warmed to 34 °C. Field excitatory postsynaptic potentials (fEPSPs) were evoked by a 0.05 Hz test stimulus through a bipolar stimulating electrode placed on the Schaffer collateral/commissural pathway and recorded from the stratum radiatum of CA1 using a glass electrode filled with 3 M NaCl. Recording was performed using a single-electrode amplifier (CEZ-3100, Nihon Kohden, Tokyo, Japan), and the maximal value of the initial fEPSP slope was recorded and averaged every 1 min (3 traces) using an A/D converter (PowerLab 200; AD Instruments, Castle Hill, NSW, Australia) and a personal computer. After a stable baseline was obtained, high frequency stimulation of 100 Hz with a 1-s duration was applied twice with a 20-s interval, and test stimuli were continued for the indicated periods.

Whole-cell patch-clamp recording. The external solution for recording whole-cell currents contained 150 mM NaCl, 5 mM KCl, 2.5 mM CaCl₂, 1 mM MgCl₂, 5.5 mM HEPES acid, 4.5 mM HEPES sodium, 10 mM D-glucose, pH 7.3 and osmolarity was adjusted to 300 mOsm with D-glucose. Ionic currents were recorded using the whole-cell patch-clamp technique at room temperature (21–22 °C). Pipette electrodes were made from 1.5-mm (outer diameter) borosilicate glass capillary tubes (Narishige, Tokyo, Japan) with a resistance of 5–10 MΩ (fabricated on a puller, Model P-97, Sutter Instruments, Novato, CA, USA) when filled with the standard internal solution, which contained 140 mM potassium-gluconate, 2 mM MgCl₂, 1 mM CaCl₂, 10 mM HEPES acid, 10 mM EGTA, 2 mM ATP-Mg²⁺ and 0.2 mM GTP-Na⁺. Membrane potentials were clamped at -80 mV unless otherwise stated. We allowed 5–10 min after membrane rupture for the cell interior to adequately equilibrate with the pipette solution. Currents through the electrode were recorded with an Axopatch-200B amplifier (Axon Instruments, Union City, CA, USA), filtered at 2 Hz, and sampled at 10 kHz using a PC-based data acquisition system that provided preliminary data analysis.

Intracellular Ca²⁺ measurement using Fura-2

N2A control and Kir6.1 or Kir6.2-overexpressing cells were cultured on glass coverslips and maintained in growth medium. After starvation in serum-free DMEM for 24-h, cells were loaded with the Ca²⁺-sensitive dye Fura-2 acetoxymethyl ester (2.5 mM) for 30 min before measurement of Ca²⁺ levels in a chamber on the stage of an inverted microscope (MetaMorph Image System; Molecular Devices, Sunnyvale, CA, USA). Cells were maintained in 1 ml Krebs-Ringer HEPES (KRH) solution (128 mM NaCl, 5 mM KCl, 2.7 mM CaCl₂, 1.2 mM Na₂HPO₄·12 H₂O, 1.2 mM MgSO₄·7H₂O, 10 mM glucose, 20 mM HEPES, pH 7.4) in the presence of memantine (10 nM), and intracellular Ca²⁺ concentrations was measured for 3 min.

Immunohistochemistry

Hippocampal primary culture. Mouse embryos were removed from 17-day pregnant C57BL/6J mice under sevoflurane anesthesia. Small wedges of hippocampus were excised and subsequently incubated in phosphate buffer solution for 20 min at 37 °C. The solution contained 154 mM NaCl, 1 mM KH₂PO₄, 3 mM Na₂HPO₄·7H₂O, 0.25% (w/v) trypsin (Type XI; Sigma-Aldrich, St. Louis, MO, USA), pH 7.4, and with osmolarity of 287 mOsm. Digested tissue was mechanically triturated by repeated passages through a Pasteur pipette, and dissociated cells were suspended in neurobasal medium with B-27 supplement (Life Technologies, Gaithersburg, MD, USA) and 2 mM glutamine. Cells were added to 35-mm culture wells at 100 000

cells ml⁻¹. Each well contained five 12-mm poly-L-lysine coated coverslips overlaid with confluent glial cells plated 2–4 weeks earlier. Cultures were maintained in a humidified atmosphere of 90% air and 10% CO₂ at 34 °C, and cells cultured 3–7 weeks were used for experiments.

Hippocampal slice. Mice were anesthetized with sevoflurane and perfused via the ascending aorta with phosphate-buffered saline (PBS; pH 7.4) until the outflow became clear. The perfusate was then switched to phosphate buffer (pH 7.4) containing 4% paraformaldehyde for 15 min. The brain was removed, post-fixed in the same solution for 24-h at 4 °C, and sliced at 50 µm using a vibratome (Leica VT1000S). Coronal sections were incubated for 30 min in PBS, 30 min in 2N HCl, 1 h in PBS with 3% bovine serum albumin (blocking solution), and then overnight in blocking solution at 4 °C with combinations of the following antibodies: rabbit anti-Kir6.1 polyclonal antibody (1:200) (made by Moriguchi *et al.*), guinea pig anti-Kir6.2 polyclonal antibody (1:200) (made by Moriguchi *et al.*), mouse anti-NeuN monoclonal antibody (1:500) (Millipore, Billerica, MA, USA), mouse anti-MAP2 monoclonal antibody (1:200) (Millipore), mouse anti-GFAP monoclonal antibody (1:400) (Sigma-Aldrich, St. Louis, MO, USA), anti-synaptophysin monoclonal antibody (1:500) (Millipore), and mouse anti-PSD-95 monoclonal antibody (1:200) (Millipore). After thorough washing in PBS, sections were incubated 3-h in Alexa 405-labeled anti-chicken, in Alexa 488-labeled anti-rat IgG or Alexa 594-labeled anti-mouse IgG. After several PBS washes, sections were mounted on slides with Vectashield (Vector Laboratories, Burlingame, CA, USA). Immunofluorescent images were analyzed using a confocal laser scanning microscope (Nikon EZ-C1, Nikon, Tokyo, Japan; JSM700, Zeiss, Thornwood, NY, USA).

Immunoblotting analysis

Hippocampal CA1 samples were homogenized in 70 µl homogenizing buffer containing 50 mM Tris-HCl (pH 7.4), 0.5% Triton X-100, 4 mM EGTA, 10 mM EDTA 1 mM Na₃VO₄, 40 mM sodium pyrophosphate, 50 mM NaF, 100 mM calyculin A 50 µg/me leupeptin, 25 µg ml⁻¹ pepstatin A 50 µg ml⁻¹ trypsin inhibitor and 1 mM dithiothreitol (DTT). Insoluble material was removed by a 10 min centrifugation at 15 000 r.p.m. After determining protein concentration in supernatants using Bradford's solution, samples were boiled 3 min in Laemmli buffer, and samples containing equivalent amounts of protein were subjected to SDS-polyacrylamide gel electrophoresis (PAGE). Proteins were transferred to an Immobilon PVDF membrane for 2-h at 70 V. After blocking with TTBS solution (50 mM Tris-HCl, pH 7.5, 150 mM NaCl and 0.1% Tween 20) containing 2.5% bovine serum albumin for 1-h at room temperature, membranes were incubated overnight at 4°C with anti-phospho CaMKII, (1:5000),¹⁸ anti-CaMKII, (1:5000),¹⁹ anti-phospho-CaMKIV (Thr-196) (1:2000, Abcam, Cambridge, MA, USA), anti-CaMKIV (1:2000, Abcam), anti-phospho-synapsin I (Ser-603) (1:2000, Millipore), anti-synapsin I (1:1000, Millipore), anti-phospho-GluA1 (Ser-831) (1:1000, Millipore), anti-GluA1 (1:1000, Millipore), anti-phospho-MAP kinase (Diphospholated ERK 1/2) (1:2000, Sigma-Aldrich), anti-MAP kinase (1:2000, Sigma-Aldrich), anti-phospho-CREB (Ser-133) (1:2000, Millipore), anti-CREB (1:2000, Millipore), anti-Kir6.1 (1:1000, made by Moriguchi *et al.*), anti-Kir6.2 (1:1000, made by Moriguchi *et al.*), and anti-β-tubulin (1:5000, Sigma-Aldrich). Bound antibodies were visualized using an enhanced chemiluminescence detection system (Amersham Life Science, Buckinghamshire, UK) and analyzed semiquantitatively using the National Institutes of Health Image program.

Immunoprecipitation

Co-immunoprecipitation of Kir6.1 or Kir6.2 with SUR1 was carried out using extracts of hippocampal CA1 region of brain. Briefly, extracts containing 60 µg protein were incubated 2-h at 4 °C with 10 µl of anti-Kir6.1 or anti-Kir6.2 antibody (made by Moriguchi *et al.*) and immunoprecipitates were captured by adding a protein A-Sepharose CL-4B suspension (50%, v/v). Immunoprecipitates were washed four times with buffer C (50 mM Tris-HCl (pH 7.5), 0.5 M NaCl, 4 mM EDTA, 4 mM EGTA, 1 mM Na₃VO₄, 50 mM NaF, 1 mM DTT, 1 mM PMSF, 2 µg ml⁻¹ pepstatin A, 1 µg ml⁻¹ leupeptin and 100 nmol L⁻¹ calyculin A), washed twice with 20 mM Tris-HCl (pH 7.5) plus 1 mM DTT, and then run on 12% acrylamide SDS-PAGE. Cell extracts and immunocomplexes precipitated were analyzed by immunoblotting as described above. Antibodies used include anti-Kir6.1 (1:500) and anti-Kir6.2 (1:500) (both made by Moriguchi *et al.*), anti-SUR1 (mouse monoclonal; 1:500; Millipore) and β-tubulin (mouse monoclonal 1:1000; Sigma-Aldrich).

Measurement of blood glucose level

We measured blood glucose levels after drug treatment using the Blood Glucose Monitoring System 'Glucose PILOT' (Aventir Biotech, Carlsbad, CA, USA).

Statistical analysis

Data are expressed as means ± s.e.m. Statistical analysis was performed using Prism 6 (Graphpad software, San Diego, CA, USA). Comparisons between two experimental groups were made using the unpaired Student's *t*-test. Statistical significance for differences among groups was tested by one-way or two-way analysis of variance, followed by a *post-hoc* Bonferroni's multiple comparison test between control and other groups. Asterisks (**P* < 0.05, ***P* < 0.01) denote statistical significance in graphs.

RESULTS

Memantine improves cognitive deficits in APP23 mice via K_{ATP} channels and CaMKII activation

APP23 mice overexpress human APP harboring the so-called 'Swedish mutation' KM670/671NL and show increased Aβ production in brain with consequent cerebral amyloidosis.^{15,20,21} We first confirmed that repeated memantine treatment (1 mg kg⁻¹, p.o.) for 28 days antagonized memory deficits seen in 12-month-old APP23 mice in terms of spatial and contextual memory using Y-maze, novel object recognition and passive avoidance tasks (Supplementary Figures S1a–e). As memory formation requires hippocampal function, we examined hippocampal long-term potentiation (LTP) in APP23 mice and found that LTP induction and maintenance was slightly but significantly improved by memantine treatment (Figures 1a and b, *post-hoc* Bonferroni multiple comparison test, *P* = 0.0294 (at 60 min)). Among K_{ATP} channel openers, pretreatment of hippocampal slices with pinacidil (3 µM) eliminated memantine-induced LTP enhancement (Figures 1a and b, *post-hoc* Bonferroni multiple comparison test, *P* = 0.0276 (at 60 min)). Memantine also altered α-amino-3-hydroxy-5-methyl-4-isoxazolepropionate receptor (AMPA) responses, as indicated by input-output relation curves showing synaptic fire volley (Figure 1c). However, unexpectedly, pinacidil treatment did not alter hippocampal LTP and input-output relation curves in wild-type mice (Supplementary Figures S2a and b). As CaMKII and Ca²⁺/calmodulin-dependent protein kinase IV (CaMKIV) mediate induction and maintenance of hippocampal LTP,^{5,20} we assessed CaMKII autophosphorylation and CaMKIV phosphorylation in CA1 after memantine treatment. Consistent with our observations of LTP impairment, CaMKII autophosphorylation and CaMKIV phosphorylation in CA1 were significantly reduced in APP23 mice relative to wild-type mice. As expected, reduced phosphorylation of CaMKII and CaMKIV seen in APP23 mice was restored by memantine treatment (Figures 1d and e, *post-hoc* Bonferroni multiple comparison test, CaMKII: *P* < 0.0001; CaMKIV: *P* < 0.0001). Pinacidil pretreatment blocked memantine effects in APP23 mice, as expected (Figures 1d and e, *post-hoc* Bonferroni multiple comparison test, CaMKII: *P* = 0.0001; CaMKIV: *P* < 0.0001). Likewise, reduced extracellular signal-regulated kinase (ERK) phosphorylation seen in APP23 mice was not rescued by memantine treatment (Figures 1d and e). Consistent with elevated hippocampal CaMKII and CaMKIV activities, phosphorylation of GluA1 (Ser-831) and CREB (Ser-133) (downstream targets of CaMKII and CaMKIV, respectively) in CA1 was also significantly decreased and rescued by memantine treatment in APP23 mice (Supplementary Figures S3a and b, *post-hoc* Bonferroni multiple comparison test, GluA1: *P* < 0.0001; CREB: *P* < 0.0001). Pretreatment with pinacidil blocked memantine-induced GluA1 and CREB phosphorylation in the APP23 mouse hippocampus (Supplementary Figures S3a and b, *post-hoc* Bonferroni multiple comparison test, GluA1: *P* < 0.0001; CREB: *P* < 0.0001). Kir6.1 or Kir6.2 protein levels also

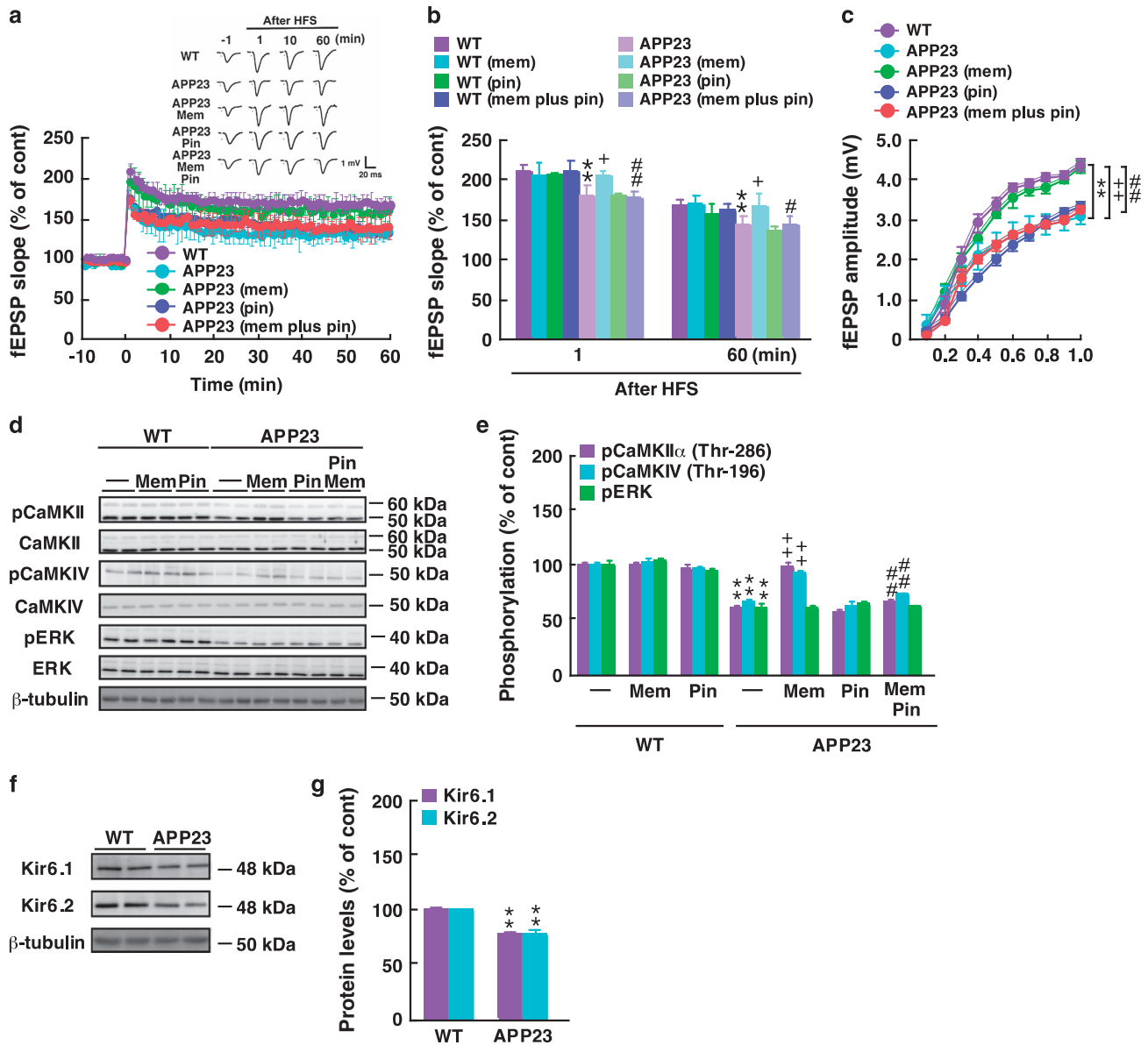


Figure 1. Memantine improves cognitive deficits in APP23 mice via CaMKII activation. **(a)** Changes in fEPSP slope following HFS recorded in CA1 were attenuated in APP23 mice, and memantine significantly ameliorated LTP impairment in that region. LTP rescue by memantine was eliminated by treatment with 3 μ M pinacidil. **(b)** Changes in fEPSP slope following HFS at 1 or 60 min in **(a)** ($n=5$ per group, 60 min: $165.8 \pm 4.1\%$ in wild-type mice versus $140.4 \pm 4.9\%$ in APP23 mice, $P=0.0042$; $140.4 \pm 4.9\%$ in APP23 mice versus $164.2 \pm 7.5\%$ in memantine-treated APP23 mice, $P=0.0294$; $164.2 \pm 7.5\%$ in memantine-treated APP23 mice versus $140.1 \pm 4.9\%$ in memantine and pinacidil-treated APP23 mice, $P=0.0276$). **(c)** Input–output relationship following high intensity stimulation of >0.1 mA. fEPSP amplitude was significantly decreased in APP23 mice but rescued by memantine treatment. Rescue of fEPSP amplitude by memantine was eliminated by treatment with 3 μ M pinacidil. ($n=8$ per group, $4.4 \pm 1.5\%$ in wild-type mice versus $3.1 \pm 0.2\%$ in APP23 mice, $P < 0.0001$; $3.1 \pm 0.2\%$ in APP23 mice versus $4.3 \pm 1.6\%$ in memantine-treated APP23 mice, $P < 0.0001$; $4.3 \pm 1.6\%$ in memantine-treated APP23 mice versus $3.3 \pm 0.8\%$ in memantine and pinacidil-treated APP23 mice, $P < 0.0001$). **(d)** Representative immunoblots of hippocampal lysates probed with antibodies recognizing autophosphorylated CaMKII α (Thr-286), CaMKII, phosphorylated CaMKIV (Thr-196), CaMKIV, phosphorylated ERK (Thr-202/Tyr-204), ERK and β -tubulin. **(e)** Quantitative analyses of data shown in **(d)**. Memantine significantly rescued decreased CaMKII α autophosphorylation (Thr-286) and CaMKIV phosphorylation (Thr-196) in CA1 of APP23 mice. CaMKII and CaMKIV activities rescued by memantine were inhibited by bath application of 3 μ M pinacidil ($n=6$ per group, CaMKII: $100.0 \pm 3.9\%$ in wild-type mice versus $68.8 \pm 2.0\%$ in APP23 mice, $P < 0.0001$; $68.8 \pm 2.0\%$ in APP23 mice versus $97.1 \pm 3.5\%$ in memantine-treated APP23 mice, $P < 0.0001$; $97.1 \pm 3.5\%$ in memantine-treated APP23 mice versus $76.5 \pm 2.7\%$ in memantine and pinacidil-treated APP23 mice, $P=0.0001$; CaMKIV: $100.0 \pm 1.6\%$ in wild-type mice versus $75.0 \pm 4.2\%$ in APP23 mice, $P < 0.0001$; $75.0 \pm 4.2\%$ in APP23 mice versus $97.2 \pm 1.4\%$ in memantine-treated APP23 mice, $P < 0.0001$; $97.2 \pm 1.4\%$ in memantine-treated APP23 mice versus $78.0 \pm 3.6\%$ in memantine and pinacidil-treated APP23 mice, $P < 0.0001$). **(f)** Representative immunoblots of hippocampal lysates from wild-type or APP23 mice probed with Kir6.1 or Kir6.2 antibodies. **(g)** Quantitative analyses showing that Kir6.1 or Kir6.2 protein levels significantly decrease in CA1 of APP23 mice ($n=8$ per group, Kir6.1: $100.0 \pm 9.2\%$ in wild-type mice versus $78.0 \pm 2.1\%$ in APP23 mice, $P < 0.0001$; Kir6.2: $100.0 \pm 1.9\%$ in wild-type mice versus $78.9 \pm 2.3\%$ in APP23 mice, $P < 0.0001$). Error bars indicate s.e.m. $**P < 0.01$ versus wild-type mice, $+P < 0.05$; $++P < 0.01$ versus APP23 mice, $\#P < 0.05$; $\#\#P < 0.01$ versus memantine-treated APP23 mice. fEPSP, field excitatory postsynaptic potentials; HFS, high frequency stimulation; LTP, long-term potentiation; WT, wild-type.

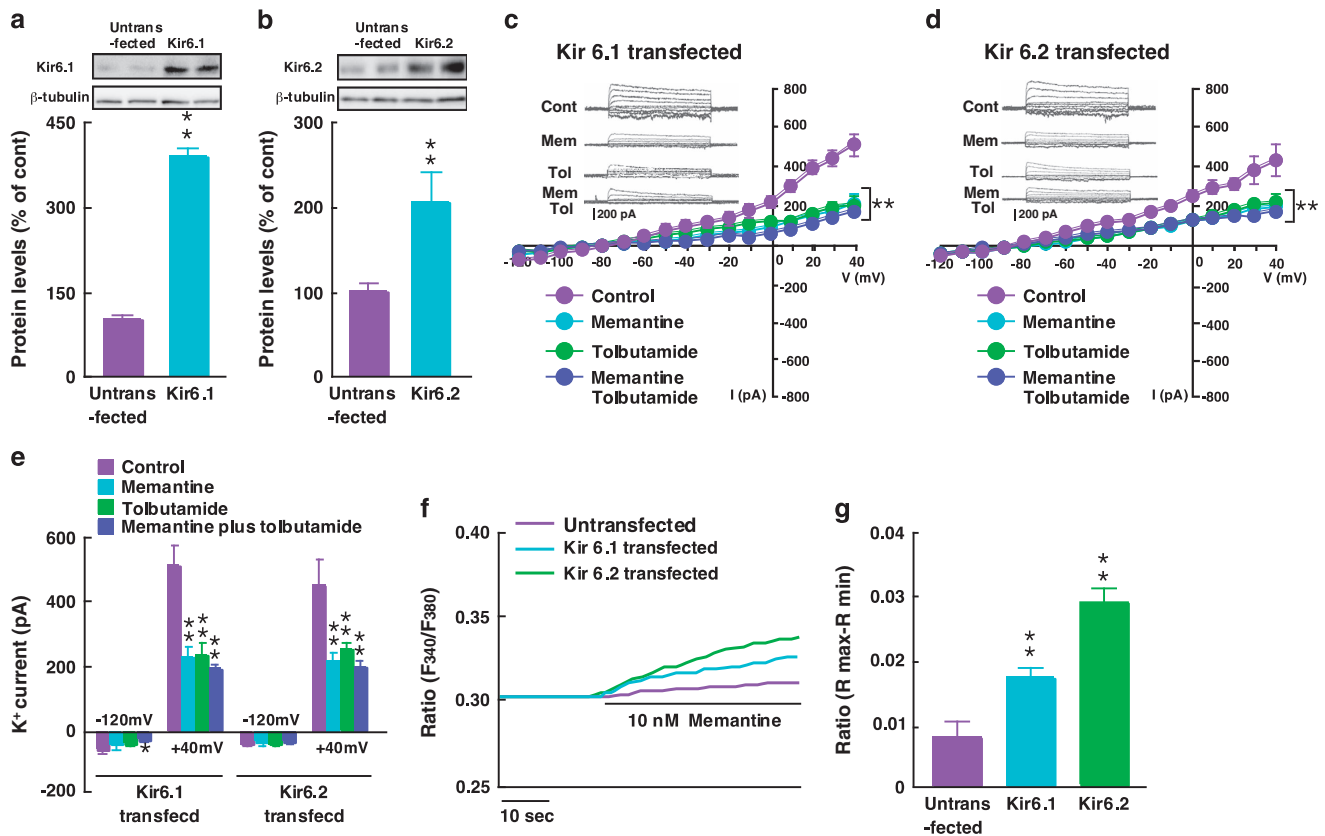


Figure 2. Memantine increases intracellular calcium levels and inhibits K⁺ currents in Kir6.1- or Kir6.2-overexpressing N2A cells. **(a,b)** Levels of overexpressed Kir6.1 **(a)** or Kir6.2 **(b)** protein in transfected and control N2A cells ($n=5$ per group). **(c,d)** Current–voltage relationships of outward K⁺ currents at holding potentials of -120 to $+40$ mV in the presence and absence of 10 nM memantine or 10 μ M tolbutamide as assessed by whole-cell recording. Memantine inhibited outward K⁺ currents in both Kir6.1- and Kir6.2-overexpressing N2A cells. Outward K⁺ currents were also inhibited by tolbutamide ($n=5$ per group, Kir6.1: memantine versus control, $P=0.0001$; tolbutamide versus control, $P=0.0002$; memantine plus tolbutamide versus control, $P<0.0001$; Kir6.2: memantine versus control, $P=0.0024$; tolbutamide versus control, $P=0.0071$; memantine plus tolbutamide versus control, $P=0.0024$). **(e)** Summary of changes in inward K⁺ currents (-120 mV) and outward K⁺ currents ($+40$ mV) in the presence and absence of 10 nM memantine or 10 μ M tolbutamide. **(f)** Changes in intracellular Ca²⁺ concentration in memantine-stimulated N2A cells. Representative traces show changes in Ca²⁺/fura-2A fluorescence induced by memantine stimulation. **(g)** Summary of changes in intracellular Ca²⁺ concentration in memantine-stimulated N2A cells overexpressing Kir6.1 or Kir6.2. Memantine stimulation increased intracellular Ca²⁺ concentration in both ($n=5$ per group, Kir6.1: $0.017 \pm 0.002\%$ in Kir6.1-transfected N2A cells versus $0.008 \pm 0.002\%$ in untransfected N2A cells, $P<0.0001$; Kir6.2: $0.029 \pm 0.002\%$ in Kir6.2-transfected N2A cells versus $0.008 \pm 0.002\%$ in untransfected N2A cells, $P<0.0001$). Error bars indicate s.e.m. ** $P<0.01$ versus control.

significantly decreased in CA1 of APP23 mice (Figures 1f and g, *post-hoc* Bonferroni multiple comparison test, Kir6.1: $P<0.0001$; Kir6.2: $P<0.0001$). Taken together, our findings indicate that memantine stimulates CaMKII and CaMKIV activities in a K_{ATP} channel-dependent manner; thus decreased Kir6.1 or Kir6.2 levels may account for impaired LTP induction and memory loss in APP23 mice.

Memantine increases intracellular calcium levels and inhibits K⁺ currents in Kir6.1- or Kir6.2-overexpressing cells

We next confirmed that memantine directly inhibits K_{ATP} channels in neurons. To do so we transiently expressed Kir6.1 or Kir6.2 in N2A cells, a manipulation that enhanced basal expression by two- to fourfold (Figures 2a and b, *post-hoc* Bonferroni multiple comparison test, Kir6.1: $P<0.0001$; Kir6.2: $P<0.0001$). Kir6.1 or Kir6.2 overexpression promoted formation of a complex with endogenous SUR1 in N2A cells (Supplementary Figures S4a and b). Using patch-clamp methods, we observed that Kir6.1 or Kir6.2 overexpression significantly increased outward K⁺ conductance. In both Kir6.1- and Kir6.2-overexpressing N2A cells, memantine

(10 nM), like the K⁺ channel blocker tolbutamide, significantly inhibited outward K⁺ currents elicited by progressive depolarizing steps from -120 to $+40$ mV from a holding potential of -80 mV seen in control cells (Figures 2c–e, Kir6.1: *post-hoc* Bonferroni multiple comparison test, $P=0.0001$, Kir6.2: $P=0.0024$). We also observed that memantine (10 nM) slightly but significantly inhibited outward K⁺ currents in Kir6.1- and Kir6.2- non-transfected N2A cells (Supplementary Figures S5a and b). Inhibition of outward K⁺ currents by memantine totally eliminated by pinacidil treatment (100 nM) (Supplementary Figures S5a and b). Kir6.1 and Kir6.2 channel inhibition elevated Ca²⁺ levels in N2A cells based on Fluo-2 Ca²⁺ imaging (Figures 2f and g, *post-hoc* Bonferroni multiple comparison test, Kir6.1: $P<0.0001$; Kir6.2: $P<0.0001$). Taken together, these findings suggest that, like tolbutamide, memantine directly inhibits neuronal SUR/Kir6.1 or SUR/Kir6.2 channels.

Kir6.2 but not Kir6.1 localizes to dendritic spines in hippocampal neurons

We next performed immunohistochemistry to define localization of hippocampal Kir6.1 or Kir6.2 protein. Although both proteins

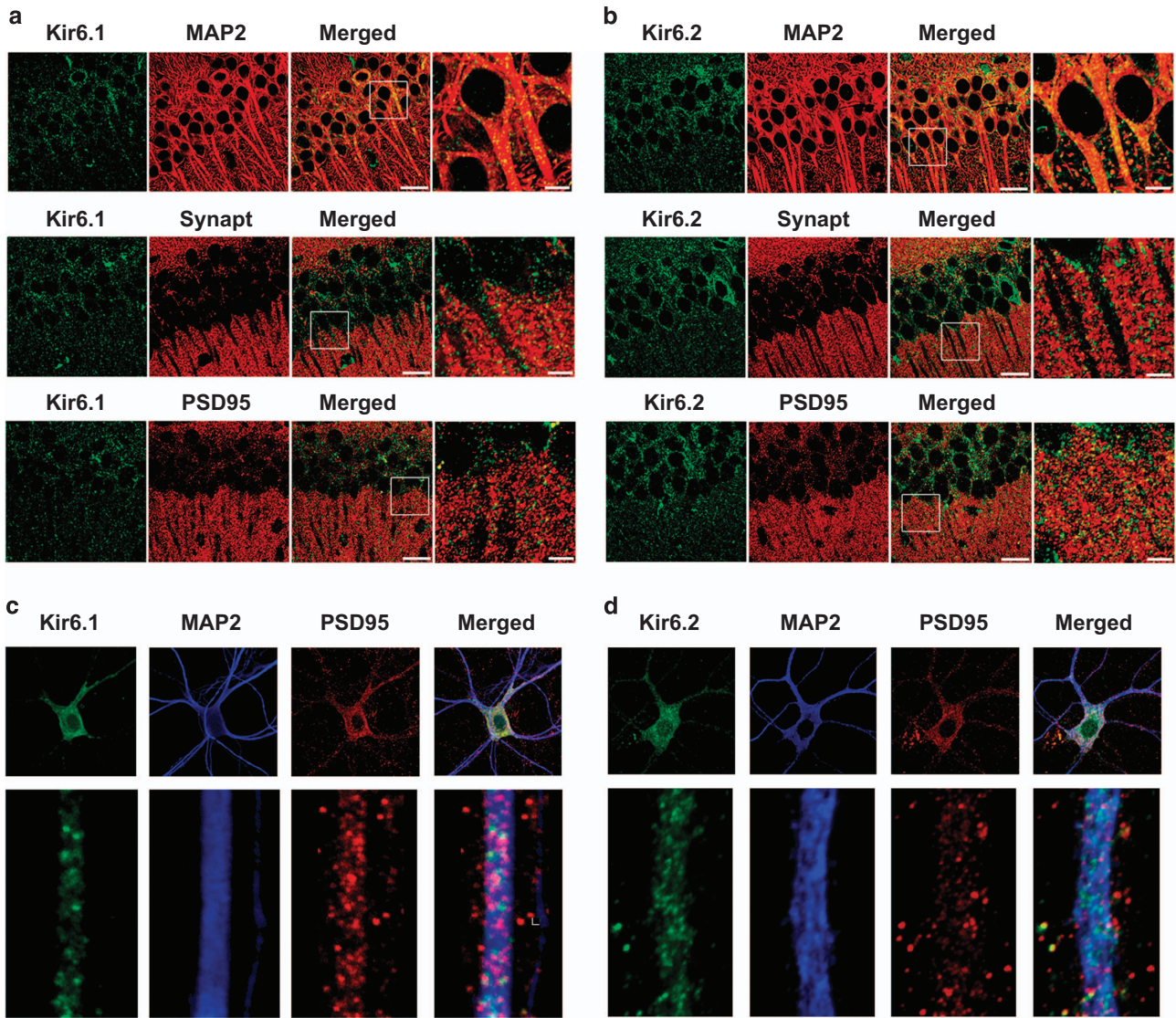


Figure 3. Kir6.2 but not Kir6.1 localizes to dendritic spines of hippocampal neurons. **(a,b)** Confocal microscopy images showing double-staining of hippocampal slices for Kir6.1 or Kir6.2 (green); MAP2, PSD-95 or synaptophysin (red); and merged images. **(c,d)** Confocal microscopy images showing triple staining of cultured hippocampal neurons for Kir6.1 or Kir6.2 (green), MAP2 (blue), and PSD-95 (red) and merged images. Kir6.2 co-localizes with PSD-95 in hippocampal neurons, but Kir6.1 does not. Scale bars, 20 μm at low magnification and 5 μm in high magnification images.

were predominantly expressed in cell bodies and apical dendrites of CA1 pyramidal neurons, Kir6.2 was also localized to distal dendrites, where it co-localized with the postsynaptic marker PSD-95 (Figures 3a and b). Similar co-localization was also observed in cultured hippocampal neurons (Figures 3c and d). Although Kir6.1 was also expressed in cell bodies and dendrites of pyramidal neurons, Kir6.1 immunoreactivity did not co-localize with that of PSD-95 in cultured pyramidal neurons (Figure 3c). Moreover, Kir6.1 was strongly expressed in GFAP-positive astrocytes in the CA1 region, cells in which Kir6.2 was only weakly expressed (Supplementary Figures S6a and b).

Memantine treatment does not improve cognitive deficits in Kir6.2 $-/-$ mice

To address potential functions of Kir6.1 and Kir6.2 in hippocampus-dependent memory formation, we assessed memory-related behaviors and hippocampal LTP in Kir6.1 or Kir6.2 loss-of-function mice. Because Kir6.1 null mice show peri-

natal lethality, we employed Kir6.1 heterozygous mutants, whereas in the case of Kir6.2, we evaluated homozygous mutants (Supplementary Figures S7a–c). Interestingly, short-term spatial memory (Figures 4a–c) and fear-conditioned contextual memory (Figures 4d and e) were largely impaired in Kir6.2 $-/-$ but not in Kir6.1 $+/-$ mice (Figures 4a–e). Repeated memantine treatment (1 mg kg^{-1}) for 28 days did not rescue memory impairment seen in Kir6.2 $-/-$ mice (Figures 4a–e). NMDAR activation is essential for LTP in the hippocampal CA1 region.^{23,24} Consistent with memory deficits, Kir6.2 $-/-$ but not in Kir6.1 $+/-$ mice exhibited impaired LTP in CA1 (Figures 4f–h, *post-hoc* Bonferroni multiple comparison test, Kir6.2: $P = 0.0074$ (at 60 min)). Similar to effects seen in behavioral tests, repeated memantine treatment did not rescue LTP deficits in Kir6.2 $-/-$ mice (Figures 4g and h). Moreover, memantine treatment had no effect on LTP induction in CA1 of Kir6.1 $+/-$ or wild-type mice (Figures 4f and h; Supplementary Figures S2a and b). Similar to Kir6.2 $-/-$ mice, Kir6.2 $+/-$ mice exhibited impaired hippocampal LTP and deficits

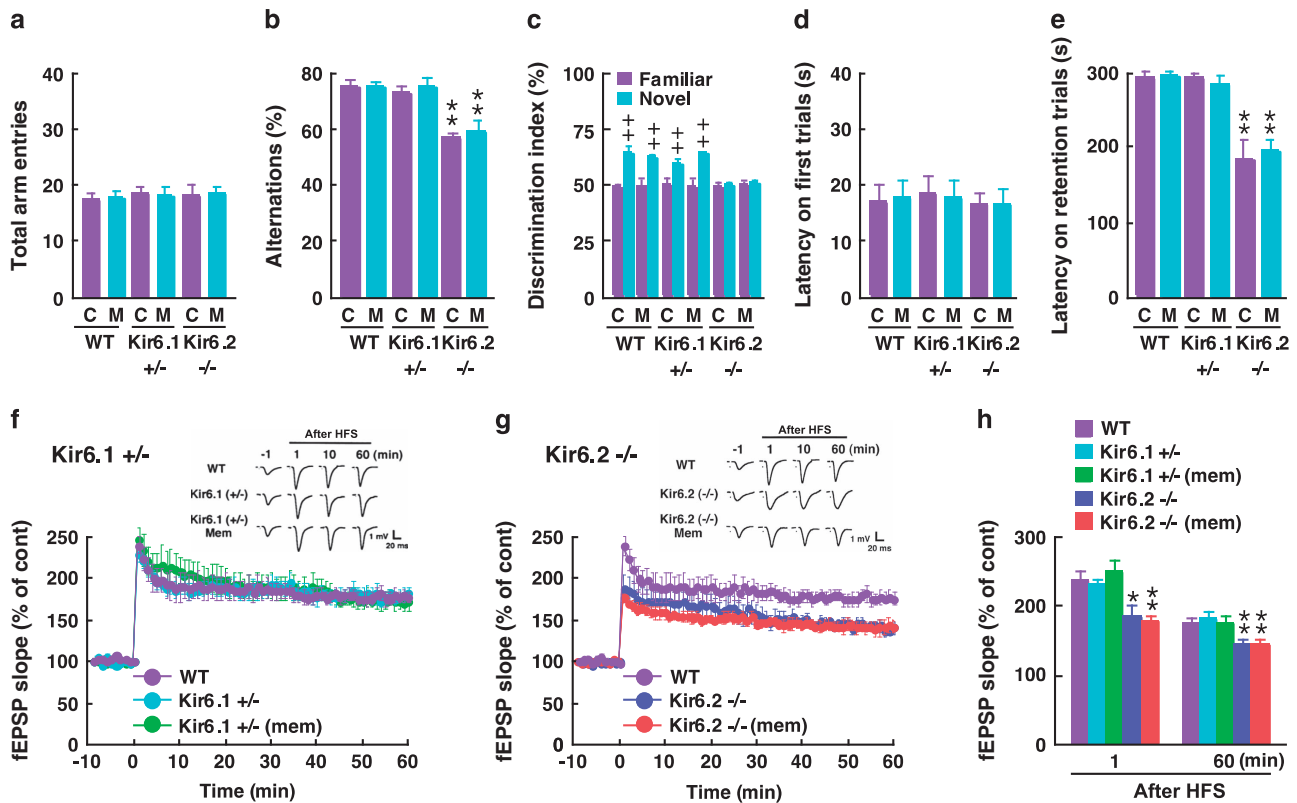


Figure 4. Memantine does not improve cognitive deficits or impaired hippocampal LTP in Kir6.2 $-/-$ mice. **(a–e)** Memory-related behavioral tests. Locomotor activity **(a)** or alternations **(b)** in a Y-maze task were measured in wild-type mice, memantine (M)-treated wild-type mice, Kir6.1 $+/-$ mice, memantine-treated Kir6.1 $+/-$ mice, Kir6.2 $-/-$ mice or memantine-treated Kir6.2 $-/-$ mice. **(c)** Mice not administered memantine. Alternation behavior in Kir6.2 $-/-$ mice significantly decreased relative to wild-type mice without changes in locomotor activity. Memantine administered to Kir6.2 $-/-$ mice at 1 mg kg^{-1} p.o. for 28 days failed to rescue alternations ($n=6$ per group, $75.4 \pm 1.9\%$ in wild-type mice versus $57.2 \pm 1.7\%$ in Kir6.2 $-/-$ mice, $P < 0.0001$; $57.2 \pm 1.7\%$ in Kir6.2 $-/-$ mice versus $59.1 \pm 3.6\%$ in memantine-treated Kir6.2 $-/-$ mice, $P = 0.5756$). **(c)** The number of times a mouse recognizes a novel object was measured between wild-type mice, memantine-treated wild-type mice, Kir6.1 $+/-$ mice, memantine-treated Kir6.1 $+/-$ mice or Kir6.2 $-/-$ mice or memantine-treated Kir6.2 $-/-$ mice. The number of times a mouse recognizes a novel object significantly decreased in Kir6.2 $-/-$ compared with wild-type mice; memantine treatment did not rescue these phenotypes ($n=6$ per group, $63.9 \pm 3.1\%$ in wild-type mice, $P < 0.0001$; $50.6 \pm 1.5\%$ in Kir6.2 $-/-$ mice, $P = 0.3584$; $50.7 \pm 1.6\%$ in memantine-treated Kir6.2 $-/-$ mice, $P = 0.5711$). **(d,e)** Latency time in first trials **(d)** and retention trials **(e)** in a passive avoidance task were measured. Latency time on retention trials in Kir6.2 $-/-$ mice significantly decreased compared with wild-type mice, and memantine treatment did not rescue this effect ($n=5$ per group, $291.6 \pm 8.4\%$ in wild-type mice versus $183.2 \pm 25.0\%$ in Kir6.2 $-/-$ mice, $P = 0.0001$; $183.2 \pm 25.0\%$ in Kir6.2 $-/-$ mice versus $195.2 \pm 14.8\%$ in memantine-treated Kir6.2 $-/-$ mice, $P = 0.5878$). **(f,g)** Changes in fEPSP slope recorded in CA1 following HFS were attenuated in Kir6.2 $-/-$ mice, and memantine failed to rescue impaired LTP in the CA1 region. By contrast, Kir6.1 $+/-$ mice show normal hippocampal LTP in CA1. **(h)** Changes in fEPSP slope following HFS at 1 or 60 min in **(f,g)** ($n=5$ per group, 60 min: $176.8 \pm 7.6\%$ in wild-type mice versus $142.2 \pm 7\%$ in Kir6.2 $-/-$ mice, $P = 0.0074$; $142.2 \pm 7\%$ in Kir6.2 $-/-$ mice versus $142.6 \pm 6.8\%$ in memantine-treated Kir6.2 $-/-$ mice, $P = 0.9638$). Error bars show s.e.m. * $P < 0.05$; ** $P < 0.01$ versus wild-type mice, +++ $P < 0.01$ versus familiar object. fEPSP, field excitatory postsynaptic potentials; HFS, high frequency stimulation; LTP, long-term potentiation; WT, wild-type.

in short-term spatial memory and/or fear-conditioned contextual memory (Supplementary Figures S8a–i).

Memantine cannot rescue impaired hippocampal LTP and cognitive deficits in CaMKII α $+/-$ mice

As memantine treatment increases phosphorylation of both CaMKII and CaMKIV, we asked which kinase was critical to rescue hippocampal LTP and memory behaviors. Notably, repeated memantine treatment (1 mg kg^{-1}) over 28 days did not improve impaired hippocampal LTP or CaMKII activity in CaMKII α $+/-$ mice (Figures 5a and b; Supplementary Figures S9a–c). Likewise, memory behaviors in these mice as assessed by Y-maze, novel object recognition and passive avoidance tasks were not improved by memantine treatment (Figures 5c–g). By contrast, CaMKIV $-/-$ mice showed normal cognitive behavior and hippocampal LTP (Supplementary Figures S10a–g), suggesting

that CaMKIV is not primarily involved in LTP induction impairment in Kir6.2 mutant mice.

DISCUSSION

Observations reported here strongly suggest that memantine inhibits neuronal K_{ATP} channels (Figure 6). We also conclude that memantine-induced memory improvement *in vivo* is likely due to inhibition of K_{ATP} channels, which then upregulates CaMKII activity in rodent hippocampus. It is generally accepted that memantine functions as a moderate blocker of the NMDAR channel, which then antagonizes glutamate toxicity in the AD brain. Acute exposure of hippocampal slices to memantine at $10\text{--}30\ \mu\text{M}$ significantly suppressed hippocampal LTP and CaMKII autophosphorylation *in vitro* (Supplementary Figures S11a–d). Acute memantine administration ($3\text{--}10\text{ mg kg}^{-1}$ i.p.) *in vivo* improved depressive-like behaviors through activation of CaMKII in wild-type mice.²⁵ On the other hand, we did not observe

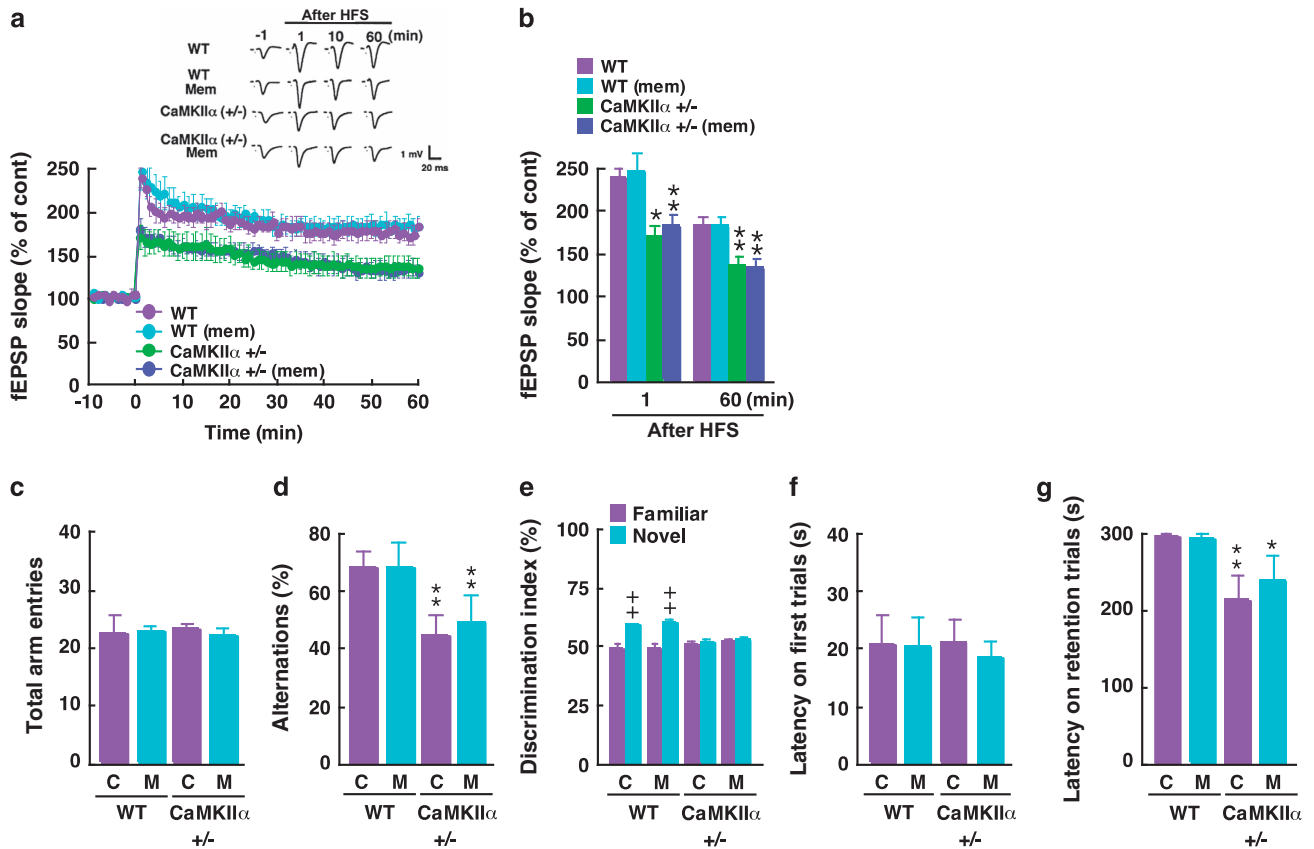


Figure 5. Memantine does not improve impaired hippocampal LTP and cognitive deficits in CaMKII α +/- mice. **(a)** Changes in fEPSP slope following HFS recorded in CA1 were attenuated in CaMKII α +/- mice and not rescued by memantine. **(b)** Changes in field excitatory postsynaptic potentials (fEPSPs) slope following HFS at 1 or 60 min, as shown in **(a)** ($n=5$ per group, 60 min: $169.2 \pm 13.5\%$ in wild-type mice versus $133.4 \pm 11.2\%$ in CaMKII α +/- mice, $P=0.0069$; $133.4 \pm 11.2\%$ in CaMKII α +/- mice versus $130.4 \pm 8.1\%$ in memantine-treated CaMKII α +/- mice, $P=0.8326$). **(c–g)** Memory-related behavioral tests. Locomotor activity **(c)** or alternation **(d)** in a Y-maze task was measured in wild-type mice, memantine-treated wild-type mice, CaMKII α +/- mice, and memantine-treated CaMKII α +/- mice. Alternations in CaMKII α +/- mice were significantly decreased relative to wild-type mice with no change in locomotor activity. Memantine administered at 1 mg kg^{-1} p.o. for 28 days did not rescue alternations in CaMKII α +/- mice ($n=5$ per group, $68 \pm 2.4\%$ in wild-type mice versus $44.7 \pm 2.7\%$ in CaMKII α +/- mice, $P < 0.0001$; $44.7 \pm 2.7\%$ in CaMKII α +/- mice versus $49.5 \pm 3.5\%$ in memantine-treated CaMKII α +/- mice, $P=0.2781$). **(e)** The number of times a mouse recognized a novel object was measured in wild-type mice, memantine-treated wild-type, CaMKII α +/-, and memantine-treated CaMKII α +/- mice. The number of times a mouse recognized a novel object in the test session significantly decreased in CaMKII α +/- relative to wild-type mice, and memantine treatment did not rescue test outcomes ($n=5$ per group, $59.6 \pm 0.6\%$ in wild-type mice, $P < 0.0001$; $51.5 \pm 0.9\%$ in CaMKII α +/- mice, $P=0.6337$; $52.4 \pm 0.8\%$ in memantine-treated CaMKII α +/- mice, $P=0.7990$). **(f–g)** Latency time in the first **(f)** and retention **(g)** trials of a passive avoidance task. Latency time on retention trials in CaMKII α +/- mice significantly decreased relative to wild-type mice, and memantine treatment did not rescue those effects on retention trials ($n=5$ per group, $294.8 \pm 3.7\%$ in wild-type mice versus $212.8 \pm 25.2\%$ in CaMKII α +/- mice, $P=0.0048$; $212.8 \pm 25.2\%$ in CaMKII α +/- mice versus $237.8 \pm 23.7\%$ in memantine-treated CaMKII α +/- mice, $P=0.4903$). Error bars show s.e.m. * $P < 0.05$; ** $P < 0.01$ versus wild-type mice, ++ $P < 0.01$ versus familiar object. HFS, high frequency stimulation; LTP, long-term potentiation; WT, wild-type.

increased CaMKII autophosphorylation following chronic administration of memantine (1 mg kg^{-1} p.o.) to wild-type mice. Therefore, CaMKII activation following K_{ATP} channel inhibition by memantine is likely detectable only in the APP23 mouse hippocampus, because those mice exhibit reduced CaMKII autophosphorylation relative to wild-type mice. Impaired Ca^{2+} homeostasis in APP23 mouse hippocampus is critical for the observation of CaMKII activation by K_{ATP} channel inhibition by memantine. Although NMDAR stimulation triggers synthesis of CaMKII α protein at postsynaptic sites,²⁶ CaMKII activation by K_{ATP} channel inhibition is likely not associated with translational activity at those sites, as here we observed no change in total CaMKII protein levels following chronic memantine administration. Thus, we conclude that hippocampal CaMKII activation is due to K_{ATP} channel inhibition.

Similarly, we have reported that loss of SK channel regulation via NMDAR in Junctophilin null mice elevates CaMKII activity in

hippocampus.¹¹ Therefore, we tested several compounds that open K^+ channels and found that pinacidil, a K_{ATP} channel opener, inhibits memantine-induced CaMKII activation in hippocampus, as shown in Figure 1. Our data also indicated that treatment with at least 100 pM memantine increases CaMKII activity in Kir6.2-overexpressing N2A cells (Supplementary Figures S12a and b). As we report here, memantine at $10\text{--}30 \text{ }\mu\text{M}$ significantly suppressed LTP and CaMKII autophosphorylation in hippocampal slices (Supplementary Figures S11a–d). Taken together, we conclude that hippocampal CaMKII activation at low doses of memantine is induced by K_{ATP} channel inhibition rather than NMDAR inhibition. Thus, we focused on Kir6.1 +/- and Kir6.2 -/- mice to assess potential pathophysiological roles of these channels in neuronal functions.

Sulfonylurea receptors are expressed ubiquitously in rodent brain²⁷ in regions where Kir6.1/Kir6.2 and SUR1 are co-expressed.²⁸ For example, Kir6.1/SUR1 complexes are the major

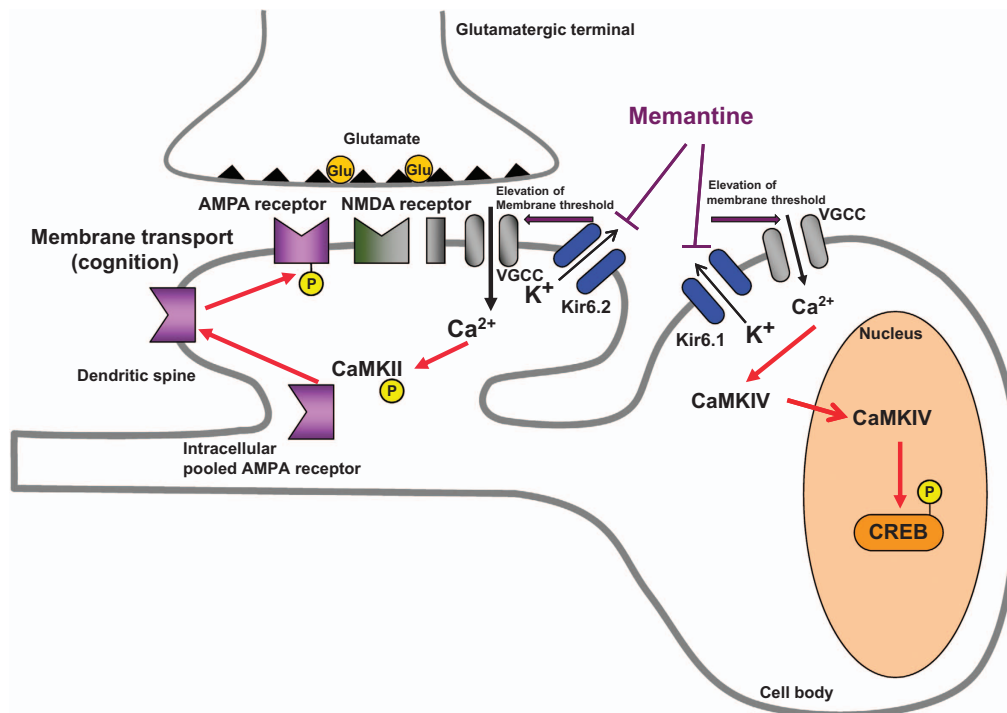


Figure 6. Proposed model for blockade of Kir6.1 or Kir6.2 by memantine in hippocampus. Our results suggest that Kir6.2 blockade in dendritic spines by memantine regulates CaMKII activity by increasing intracellular Ca²⁺ mobilization, which in turn improves cognitive function by promoting AMPAR trafficking into the postsynaptic membrane. By contrast, Kir6.1 blockade by memantine regulates CaMKIV and CREB activities via increased intracellular Ca²⁺ mobilization, an activity correlated with adult hippocampal neurogenesis. AMPAR, α -amino-3-hydroxy-5-methyl-4-isoxazolepropionate receptor; NMDA, *N*-methyl-D-aspartate.

SUR components of CA1 pyramidal cells and interneurons.²⁸ Notably, Kir6.1 and Kir6.2 are highly expressed in neurons, whereas Kir6.1 is also expressed in astrocytes.^{9,10} Although neurons reportedly exhibit glucose-regulated excitability through SUR/Kir, the functions of SUR/Kir complexes in cognition have not been addressed. In 2000, Seino *et al.*²⁹ extensively analyzed diverse functions of K_{ATP} channels in peripheral tissues using Kir6.2 $-/-$ mice. Moreover, studies of Kir6.1 heterozygous (Kir6.1 $+/-$) mice revealed impaired dentate gyrus neurogenesis.³⁰ Kir6.1 but not Kir6.2 is predominantly expressed in adult neural stem cells.³⁰ Few studies have assessed K_{ATP} channel function in memory formation of adult brain. For example, Kir6.2 $-/-$ mice show moderately impaired spatial memory by 12 weeks of age.³¹ Injection of diazoxide, a K_{ATP} channel opener, into hippocampal CA3 region impairs contextual memory in wild-type mice.³² Here, we defined the precise localization of Kir6.1 and Kir6.2 proteins in hippocampal CA1 neurons and assessed their relevance to cognition using Kir6.1 $+/-$ and Kir6.2 $-/-$ mice.

Although Kir6.1 is expressed in neuronal cell bodies and dendrites in CA1, hippocampal LTP in Kir6.1 heterozygotes was comparable to that of wild-type mice. Like Kir6.1, Kir6.2 is also expressed in neuronal cell bodies and dendrites, although its expression is particularly high at postsynaptic densities in CA1; nonetheless, Kir6.2 $-/-$ mice show moderate LTP impairment, as reflected by previous reports of behavioral deficits in novel object recognition and contextual memory tasks.³¹ In this context, predominant postsynaptic localization of Kir6.2 may be relevant to LTP induction and hippocampus-dependent memory.

Our study provides evidence that Kir6.2 is a relevant memantine target and that Kir6.2 inhibition improves cognition. Taken together, memantine treatment elevated intracellular by inhibiting outward K⁺ currents in N2A cells overexpressing either Kir6.1 or Kir6.2. Pinacidil treatment eliminated CaMKII activation by

memantine in APP23 mice. We also determined that the SUR antagonist tolbutamide elicits effects similar to memantine in N2A cells overexpressing Kir6.1 or Kir6.2. A previous study reported that the K_{ATP} channel inhibitor HMR-1372, or glibenclamide, slightly enhances hippocampal LTP induced by strong stimuli.³³ We conclude that memantine enhances Ca²⁺ mobilization by inhibiting SUR/Kir complexes, enhancing hippocampal LTP.

Although Kir6.1 and Kir6.2 channel activities were suppressed by memantine *in vitro*, LTP enhancement was not seen in Kir6.2 $-/-$ mice. However, it remains unknown how Kir6.2 activity regulates LTP establishment. One explanation is derived from the observation that CaMKII-dependent Kir6.2 phosphorylation (at T224) inhibits K_{ATP} channel activity in pancreatic β cells.³⁴ In addition, CaMKII activation promotes cell surface expression of Kir6.2 in cardiomyocytes.³⁵ However, Kir6.1 may still function in cognition, as it is enriched in CA1 neuronal cell bodies and dendrites and functions in adult neurogenesis³⁰ (Supplementary Figures S13a–d). Taken together, K_{ATP} channels play physiological roles in memory formation in adult brain, and pharmacological manipulation of K_{ATP} channels alters synaptic transmission and neuronal excitability in hippocampus. Further studies are required to define how CaMKII, NMDARs and Kir6.2 govern hippocampal synaptic plasticity.

Although we observed increased CaMKIV phosphorylation following memantine treatment, CaMKIV activity apparently does not function in hippocampus-dependent memory, as CaMKIV null mice do not show impaired LTP. By contrast, memantine increases adult hippocampal neurogenesis in wild-type mice³⁶ but fails to do so in CaMKIV null mice (Supplementary Figures S14a–d).³⁷ Thus, memantine may enhance adult hippocampal neurogenesis via Kir6.1/CaMKIV pathways.

Changes in diabetes-related genes in the AD brain have been reported, and Kir6.1 and Kir6.2 have not been included among genes abnormally regulated in AD brain.¹² In addition, Akhtar

et al.³⁸ reported that like the AD brain, type 2 diabetes mellitus in mice increases in neuronal Ca²⁺ and nitric oxide in an NMDAR-dependent manner, elevating Aβ and promoting mitochondrial dysfunction. Memantine therefore improves the NMDAR-dependent pathology. Here, we suggest that K_{ATP} channels represent other targets of memantine in addition to NMDARs. Enhanced CaMKII function following elevation of postsynaptic Ca²⁺ by K_{ATP} channel inhibition promotes synaptic plasticity and memory. Furthermore, like tolbutamide, chronic treatments with memantine decreased blood glucose levels in ob/ob diabetes model mice (Supplementary Figure S15). Thus, memantine could exert beneficial activities on both cognition and diabetic syndromes in AD patients. Its clinical usage could be highly advantageous in mild to moderate AD patients, as memantine promoted K_{ATP} channel inhibition at low doses *in vitro*.

Four weeks after ibotenic acid-induced lesioning of the nucleus basalis magnocellularis (the origin of cholinergic neurons) Kir6.1 and Kir6.2 expression reportedly increases.³⁹ Moreover, various mutations in SUR and Kir genes are thought to be a common cause of type II diabetes, among the gene that encodes Kir6.2, *KCNJ11*, which when mutant is the most common cause of neonatal diabetes.⁴⁰ Slingerland et al.⁴¹ first reported that *KCNJ11* mutation-associated cognitive impairment was improved by treatment of patients with the SUR antagonist glibenclamide. Accordingly, memantine could be an attractive therapeutic to treat cognitive impairment in AD patients with diabetes. This hypothesis could be tested by epidemiological studies of AD patients with or without diabetes, before and after treatment with SUR therapeutics.

CONFLICT OF INTEREST

The authors declare no conflict of interest.

ACKNOWLEDGMENTS

This work was supported in part by grants from the Ministry of Education, Culture, Sports, Science and Technology, and the Ministry of Health and Welfare of Japan (22390109 to KF; 20790398 to SM). Also, thanks to Professor Tsuyoshi Miyakawa for providing CaMKIIa +/- mice and Professor Susumu Seino for providing Kir6.1 +/- and Kir6.2 -/- mice. We also thank Novartis Pharma for providing APP23 mice.

AUTHOR CONTRIBUTIONS

SM, NS, HT, YY, YS, and HS performed the experiments. TI and HY provided recombinant Kir6.1 or Kir6.2. H.S. provided knockout mice. JZY and TN provided critical reagents and advice. SM and KF wrote the manuscript and designed the study.

REFERENCES

- Greenamyre JT, Penney JB, D'Amato CJ, Young AB. Dementia of the Alzheimer's type: changes in hippocampal L-[3H] glutamate binding. *J Neurochem* 1987; **48**: 543–551.
- Chen HS, Lipton SA. The chemical biology of clinically tolerated NMDA receptor antagonists. *J Neurochem* 2006; **97**: 1611–1626.
- Chen HS, Pellegrini JW, Aggarwal SK, Lei SZ, Warach S, Jensen F et al. Open-channel block of N-methyl-D-aspartate (NMDA) responses by memantine: therapeutic advantage against NMDA receptor-mediated neurotoxicity. *J Neurosci* 1992; **12**: 4427–2236.
- Lipton SA. Paradigm shift in NMDA receptor antagonist drug development: molecular mechanism of uncompetitive inhibition by memantine in the treatment of Alzheimer's disease and other neurologic disorders. *J Alzheimers Dis* 2004; **6**: S61–S74.
- Fukunaga K, Stoppini L, Miyamoto E, Muller D. Long-term potentiation is associated with an increased activity of Ca²⁺/calmodulin-dependent protein kinase II. *J Biol Chem* 1993; **268**: 7863–7867.
- Silva AJ, Paylor R, Wehner JM, Tonegawa S. Impaired spatial learning in alpha-calcium-calmodulin kinase II mutant mice. *Science* 1992; **257**: 206–211.

- Babenko AP, Aguilar-Bryan L, Bryan J. A view of sur/KIR6.X, KATP channels. *Annu Rev Physiol* 1998; **60**: 667–687.
- Zawar C, Plant TD, Schirra C, Konnerth A, Neumcke B. Cell-type specific expression of ATP-sensitive potassium channels in the rat hippocampus. *J Physiol* 1999; **514**: 327–341.
- Thomzig A, Laube G, Pruss H, Veh RW. Pore-forming subunits of K-ATP channels, Kir6.1 and Kir6.2, display prominent differences in regional and cellular distribution. *J Comp Neurol* 2005; **484**: 313–330.
- Sun XL, Hu G. ATP-sensitive potassium channels: a promising target for protecting neurovascular unit function in stroke. *Clin Exp Pharmacol Physiol* 2010; **37**: 243–252.
- Moriguchi S, Nishi M, Komazaki S, Sakagami H, Miyazaki T, Masumiya H et al. Functional uncoupling between Ca²⁺ release and afterhyperpolarization in mutant hippocampal neurons lacking junctophilins. *Proc Natl Acad Sci USA* 2006; **103**: 10811–10816.
- Hokama M, Oka S, Leon J, Ninomiya T, Honda H, Sasaki K et al. Altered expression of diabetes-related genes in Alzheimer's disease brains: the Hisayama study. *Cerebral Cortex* 2014; **24**: 2476–2488.
- Miki T, Nagashima K, Tashiro F, Kotake K, Yoshitomi H, Tamamoto A et al. Defective insulin secretion and enhanced insulin action in KATP channel deficient mice. *Proc Natl Acad Sci USA* 1998; **95**: 10402–10406.
- Miki T, Suzuki M, Shibasaki T, Uemura H, Sato T, Yamaguchi K et al. Mouse model of Prinzmetal angina by disruption of the inward rectifier Kir6.1. *Nat Med* 2002; **8**: 466–472.
- Sturchler-Pierrat C, Abramowski D, Duke M, Wiederhold KH, Mistl C, Rothacher S et al. Two amyloid precursor protein transgenic mouse models with Alzheimer's disease-like pathology. *Proc Natl Acad Sci USA* 1997; **94**: 13287–13292.
- Yamasaki N, Maekawa M, Kobayashi K, Kajii Y, Maeda J, Soma M et al. Alpha-CaMKII deficiency causes immature dentate gyrus, a novel candidate endophenotype of psychiatric disorders. *Mol Brain* 2008; **1**: 6.
- Takao K, Tanda K, Nakamura K, Kasahara J, Nakao K, Katsuki M et al. Comprehensive behavioral analysis of calcium/calmodulin-dependent protein kinase IV knockout mice. *PLoS ONE* 2010; **5**: e9460.
- Fukunaga K, Muller D, Miyamoto E. Increased phosphorylation of Ca²⁺/calmodulin-dependent protein kinase II and its endogenous substrates in the induction of long term potentiation. *J Biol Chem* 1995; **270**: 6119–6124.
- Fukunaga K, Horikawa K, Shibata S, Takeuchi Y, Miyamoto E. Ca²⁺/calmodulin-dependent protein kinase II-dependent long-term potentiation in the rat suprachiasmatic nucleus and its inhibition by melatonin. *J Neurosci Res* 2002; **70**: 799–807.
- Sturchler-Pierrat C, Staufenbiel M. Pathogenic mechanisms of Alzheimer's disease analyzed in the APP23 transgenic mouse model. *Ann NY Acad Sci* 2000; **920**: 134–139.
- Rossor MN, Newman S, Frackowiak RS, Lantos P, Kennedy AM. Alzheimer's disease families with amyloid precursor protein mutations. *Ann NY Acad Sci* 1993; **695**: 198–202.
- Kasahara J, Fukunaga K, Miyamoto E. Activation of calcium/calmodulin-dependent protein kinase IV in long term potentiation in the rat hippocampal CA1 region. *J Biol Chem* 2001; **276**: 24044–24050.
- Bliss TV, Collingridge GL. A synaptic model of memory: long-term potentiation in the hippocampus. *Nature* 1993; **361**: 31–39.
- Shi SH, Hayashi Y, Petralia RS, Zaman SH, Wenthold RJ, Svoboda K et al. Rapid spine delivery and redistribution of AMPA receptors after synaptic NMDA receptor activation. *Science* 1999; **284**: 1811–1816.
- Scheetz AJ, Nairn AC, Constantine-Paton M. NMDA receptor-mediated control of protein synthesis at developing synapses. *Nat Neurosci* 2000; **3**: 211–216.
- Almeida RC, Souza DG, Soletti RC, Lopez MG, Rodrigues ALS, Gabilan NH. Involvement of PKA, MAPK/ERK and CaMKII, but not PKC in the acute antidepressant-like effect of memantine in mice. *Neurosci Lett* 2006; **395**: 93–97.
- Zini S, Tremblay E, Pollard H, Moreau J, Ben-Ari Y. Regional distribution of sulfonylurea receptors in the brain of rodent and primate. *Neuroscience* 1993; **55**: 1085–1091.
- Karschin C, Ecker C, Ashcroft FM, Karschin A. Overlapping distribution of K_{ATP} channel-forming Kir6.2 subunit and the sulfonylurea receptor SUR1 in rodent brain. *FEBS Lett* 1997; **401**: 59–64.
- Seino S, Iwanaga T, Nagashima K, Miki T. Diverse roles of K_{ATP} channels learned from Kir6.2 genetically engineered mice. *Diabetes* 2000; **49**: 311–318.
- Yang JZ, Huang X, Zhao FF, Xu Q, Hu G. Iptakalim enhances adult mouse hippocampal neurogenesis via opening Kir6.1-composed K-ATP channels expressed in neural stem cells. *CNS Neurosci Ther* 2012; **18**: 737–744.
- Choeiri C, Staines WA, Miki T, Seino S, Renaud JM, Teutenberg K et al. Cerebral glucose transporters expression and spatial learning in the K-ATP Kir6.2 -/- knockout mice. *Behav Brain Res* 2006; **172**: 233–239.

- 32 Betourne A, Bertholet AM, Labroue E, Halley H, Sun HS, Lorisignol A *et al*. Involvement of hippocampal CA3 K_{ATP} channels in contextual memory. *Neuropharmacology* 2009; **56**: 615–625.
- 33 Schroder UH, Hock FJ, Wirth K, Englert HC, Reymann KG. The ATP-regulated K^+ -channel inhibitor HMR-1372 affects synaptic plasticity in hippocampal slices. *Eur J Pharmacol* 2004; **502**: 99–104.
- 34 Kline CF, Wright PJ, Koval OM, Zmuda EJ, Johnson BL, Anderson ME *et al*. β IV-spectrin and CaMKII facilitate Kir6.2 regulation in pancreatic beta cells. *Proc Natl Acad Sci USA* 2013; **110**: 17576–17581.
- 35 Sierra A, Zhu Z, Sapay N, Sharotri V, Kline CF, Luczak ED *et al*. Regulation of cardiac ATP-sensitive potassium channel surface expression by calcium/calmodulin-dependent protein kinase II. *J Biol Chem* 2013; **288**: 1568–1581.
- 36 Ishikawa R, Kim R, Namba T, Kohsaka S, Uchino S, Kida S. Time-dependent enhancement of hippocampus-dependent memory after treatment with memantine: Implications for enhanced hippocampal adult neurogenesis. *Hippocampus* 2014; **24**: 784–793.
- 37 Moriguchi S, Sakagami H, Yabuki Y, Sasaki Y, Izumi H, Zhang C *et al*. Stimulation of sigma-1 receptor ameliorates depressive-like behaviors in CaMKIV null mice. *Mol Neurobiol* 2015; **52**: 1210–1222.
- 38 Akhtar MW, Sanz-Blasco S, Dolatabadi N, Parker J, Chon K, Lee MS *et al*. Elevated glucose and oligomeric β -amyloid disrupt synapses via a common pathway of aberrant protein S-nitrosylation. *Nat Commun* 2016; **7**: 10242.
- 39 Xu XH, Pan YP, Wang XL. mRNA expression alterations of inward rectifier potassium channels in rat brain with cholinergic impairment. *Neurosci Lett* 2002; **322**: 25–28.
- 40 Gloyn AL, Pearson ER, Antcliff JF, Proks P, Bruining GJ, Slingerland AS *et al*. Activating mutations in the gene encoding the ATP-sensitive potassium-channel subunit Kir6.2 and permanent neonatal diabetes. *N Engl J Med* 2004; **350**: 1838–1849.
- 41 Slingerland AS, Hurkx W, Noordam K, Flanagan SE, Jukema JW, Meiners LC *et al*. Sulphonylurea therapy improves cognition in a patient with the V59M KCNJ11 mutation. *Diabetes Med* 2008; **25**: 277–281.

Supplementary Information accompanies the paper on the *Molecular Psychiatry* website (<http://www.nature.com/mp>)